RIFT results for GW170729 with higher modes: results and result stability investigations

R. O'Shaughnessy and Jacob Lange
Center for Computational Relativity and Gravitation, Rochester Institute of Technology, Rochester, New York 14623, USA

A companion paper [1] presented RIFT results for parameter inference for GW170729 with higher modes, computed using a variety of waveform models including numerical relativity, showing these results are in good agreement with one another. The RIFT analyses with HM are in modest tension with corresponding results computed with another parameter inference code (`LALInference`) when using similar settings. In this document, we describe the RIFT results, and investigations to assess their reliability. After exhaustive testing of our HM analyses specifically, particularly via extensive tests with SEOBNRv4HM, we know of no concrete reason to doubt the RIFT HM results.

I. INTRODUCTION

The Advanced LIGO [2] and Virgo [3] ground-based gravitational wave (GW) detectors have identified several coalescing compact binaries [4–9]. The properties of the sources responsible have been inferred via Bayesian comparison of each source with candidate gravitational wave signals [4–13]. Many more are expected as observatories reach design sensitivity [14]. Both to handle the rapid pace of discovery and particularly to enable coordinated multimessenger followup, GW observatories hope to reconstruct the evidence for a signal being present in the data along with the full source parameters of coalescing binaries as fast as possible [15–17]. The RIFT/rapidPE strategy described in [11, 12, 18, 19] can perform these inferences quickly and low computational cost, even for computationally costly models, without additional intermediate approximations (e.g. surrogates, reduced-order quadrature) and their requisite development and tuning; see, e.g., [20] for discussion and demonstrations of RIFT performance. The RIFT code and tutorials are publicly available [20, 21].

GW170729 is a high-mass, low-amplitude binary black hole [10]. Gravitational wave emission from BBH can be described as a sum over angular modes $h(t) = \sum_{lm} Y^{-2}_{lm} h_{lm}$, with often-subdominant terms in the sum not arising from $l = |m| = 2$ (corresponding to the mass and current quadrupole in near-flat space) known colloquially as "higher modes". The first published investigations of this event were performed with RIFT, via direct comparison to numerical relativity [19] and to NR-calibrated surrogates [22–24], as part of coordinated PE with HM on all O1 and O2 events [10, 25]. Perhaps surprisingly [26, 27], despite its low amplitude and signal brevity, some posterior inferences about GW170729 are noticibly influenced by the incorporation of higher modes. Higher modes have been previously demonstrated to impact the interpretation of GW150914; see, e.g., [19]. In both cases, HM effects do not produce substantial changes relative to the still-large statistical error. But in both cases, higher-mode effects are large enough that, in the immediate future, their neglect would impact the interpretation of a subpopulation of similar objects. Thus, these two cases demonstrate that HM can have an astrophysically interesting impact on the interpretation of even the first few observed GW sources. Particularly because extreme sources like GW170729 can have influence astrophysical interpretation of the BBH population – being already at the margins of the mass, mass ratio, spin distribution – and because the combination of multiple sources can exacerbate systematic biases present in the interpretation of any individual source, it is particularly important to perform analysis of sources like GW170729 with our best-available understanding of general relativity.

Recently, Chatziioannou and collaborators [1] (ourselves included) conducted a follow-on investigation to report more detail about this event and the impact of HM in particular. These investigations included not only reproducing the RIFT analysis described above, but also calculations with `LALInference`, a well-developed GW parameter-inference code. Additionally, benefiting from recent developments in waveform coding and internal validation, these investigations also used two new approximate waveform families: IMRPhenomHM [28] and SEOBNRv4HM [29]. This investigation therefore provided a rare opportunity to compare model-based parameter inference using both LI and HM to model-based parameter inference using RIFT and HM on real data and in a production environment. Despite a track record of good agreement for several approximations, including analyses of this event, the two codes do show mild tension between results using HM with $L > 2$. This technical document provides a detailed summary and investigation of the RIFT HM results, as a companion to Chatziioannou et al [1].

In Section II, we review the RIFT results with HM and salient differences from LI results, as reported in the Appendix of [1]. In Section III, we describe several end-to-end reanalyses performed with different code settings and inputs, almost exclusively with RIFT, providing a detailed internal self-consistency test that the RIFT results were stable to code settings. In Section IV, we describe additional investigations we performed to validate the RIFT code. Despite these investigations, we have not identified any cause to doubt the RIFT results presented here, nor an explanation for the discrepancy between RIFT and LI results with HM for GW170729.

II. RESULTS

The Appendix of [1] provides a numerical summary of the RIFT results for GW170729 using SEOBNRv4HM, NR, and NR/NRsurrogate-based PE. Figure 1 provides a graphical representation of these results. For comparison and to visually highlight the differences seen between the two codes, the sec-

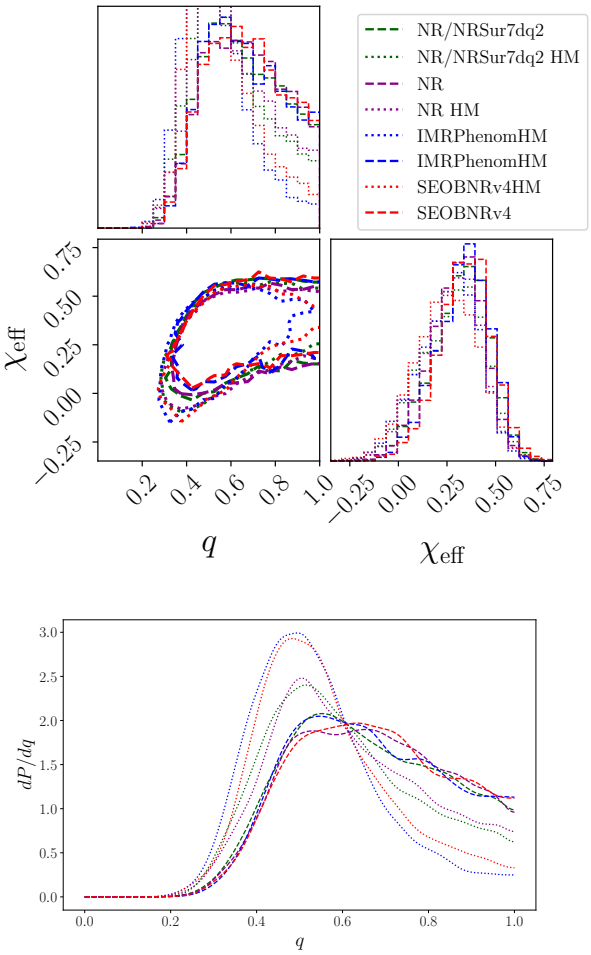

FIG. 1: RIFT results for 170729 without and with HM, for the fiducial "zprior". *Top panel*: RIFT-only results with and without HM. Results with HM are in good agreement for all three techniques used with RIFT; results without HM are in good agreement between all codes and approximations. *Bottom panel*: The one-dimensional marginal mass ratio distribution for q, showing models with only $L = 2$ modes as dashed lines and models with some $L > 2$ modes as dotted lines. LI results are taken from [1]. Comparing the two sets of dotted lines between the RIFT results and the LI results identifies differences when HM are employed.

ond panel of this figure compares the NR and NR-surrogate RIFT results to corresponding LI results for all other models. While results using only $L = 2$ modes show good agreement, calculations with HM included are not completely consistent.

All subsequent tests described in this work use similar settings to the RIFT analyses described in [1].

III. REANALYSES WITH ALTERNATIVE SETTINGS

RIFT and LI are two independently-implemented parameter estimation codes, with different data handling; likelihood implementations; and algorithm. Despite these differences, in our own internal investigations with several approximants which lack HM (e.g., SEOBNRv3, IMRPhenomD) and in several previous studies, results from these two independent approaches have been in good agreement for comparable data and using identical waveform models. In this investigation, however, the RIFT analyses using SEOBNRv4HM (shown in figure 1 do not precisely reproduce the inferred distributions from LI using the same waveform model. While both codes draw the largely similar conclusions, particularly for the other binary parameters, the LI analysis slightly favors unequal mass over RIFT inferences.

To investigate potential sources for these small differences, we conducted extensive tests for this event, repeating their analysis end-to-end with RIFT many times. As demonstrated in other studies [30], we demonstrated RIFT results do not depend on details of the NR simulation grid used (e.g., as demonstrated by the agreement between RIFT results from SEOBNRv4HM, pure NR, and NR/NRSur). We demonstrated that removing Virgo from the analysis did not change RIFT results. We demonstrated that RIFT results do not depend on the coordinate fitting strategy, by adopting alternative choices of fit coordinates; see Figure 4. This test, along with good agreement using non-HM models, precludes the possibility that the underlying priors were implemented incorrectly. We demonstrated that RIFT results do not depend on the noise power spectrum model, by reproducing the analysis using several different proposed BayesWave [31] noise power spectra drawn from different durations of data, as well as with an off-source PSD; see Figure 5. We demonstrated that RIFT results do not seem to depend on the data handling adopted, by using different amounts of data selected and different data handling; see Figure 3. (RIFT by default employs a much larger data buffer, and uses inverse spectrum truncation; however, RIFT results using LI-style data intervals and Tukey windowing were indistinguishable from our results). We demonstrated that RIFT results do not depend on the data sampling rate used in the analysis. We demonstrated that RIFT results do not depend on the waveform duration assumed, adopting several different starting frequencies for template generation; see Figure 6. (Additionally. the NR analysis always uses the full NR simulated waveform, and therefore is not subject to startup transients.) We demonstrated that RIFT results do not depend on the accuracy of Monte Carlo integration. (All RIFT marginalized likelihood evaluations are evaluated twice, to insure the possibility of retrospective consistency checks. We checked the individual data points agreed.) Finally, because RIFT assumes perfect calibration, the group demonstrated that LI results for SEOBNRv4HM did not depend on whether or not LI marginalized over calibration error, by performing a LI analysis in which calibration error marginalization was disabled.

IV. CODE TESTS

The RIFT team also did a detailed investigation of its code. They checked the waveform interface to models with HM in general (and SEOBNRv4HM in particular) was used correctly and consistent with the code path used by LI. Because of

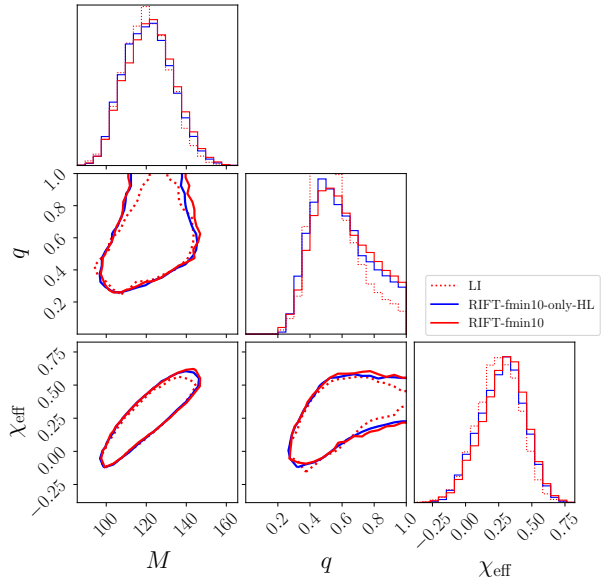

FIG. 2: RIFT analysis stability investigations: omitting Virgo. Because the Virgo data was the most feature-rich, with the most complicated PSD, we reanalyzed GW170729 without any Virgo data, to assess whether some problem with RIFT Virgo data handling might have changed the result. This change produces very modest changes relative to our fiducial analysis, at the margins of our ability to resolve with current sampling. These changes are not sufficient to perturb the mass ratio distribution, relative to the changes needed to reproduce the LI result.

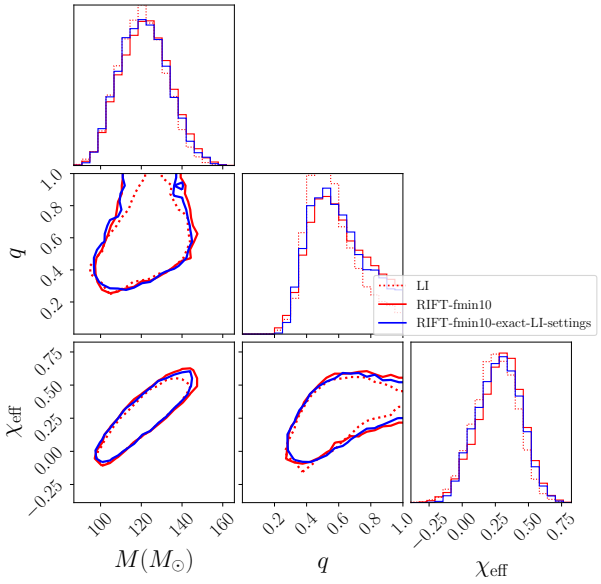

FIG. 3: RIFT analysis stability investigations: data handling. RIFT normally uses a longer data analysis window (set by the signal duration, with considerable padding on either side), not the 4s window fixed for use by LI. RIFT also uses different data conditioning methods. We adopted as close as RIFT can achieve to the data handling used by LI. This change produces very modest changes relative to our fiducial analysis, at the margins of our ability to resolve with current sampling. These changes are not sufficient to perturb the mass ratio distribution, relative to the changes needed to reproduce the LI result

the significantly-bimodal arrival time distribution for 170729 when HM were present, they checked that the time window used for likelihood marginalization always contained all relevant support.

In parallel to a related study [20], they checked the low-level likelihood code with multiple independent implementations of Eq. (A7), confirming agreement to roundoff-level error. Because one of the implementations involved complete reimplementation of every low-level function used by the likelihood (e.g., the spin-weighted spherical harmonics, arrival time, inner products, et cetera), and because several of these steps involved careful unit test (e.g., the spin-weighted spherical harmonics), we are confident the low-level likelihood code is correct.

V. CONCLUSIONS

After all these investigations, we have not been able to identify any mechanism which changes the RIFT HM results to precisely agree with the LI HM results, or indeed to change them at all. We point out that in one previous work [32], RIFT results for GW170817 were also mildly incongruent with the corresponding LI results, in that case for IMRPhenomD_NRTidal. Given considerable experience with both LI and RIFT, we appreciate that true errors can conceivably be present and remain undetected, both in these codes and in how

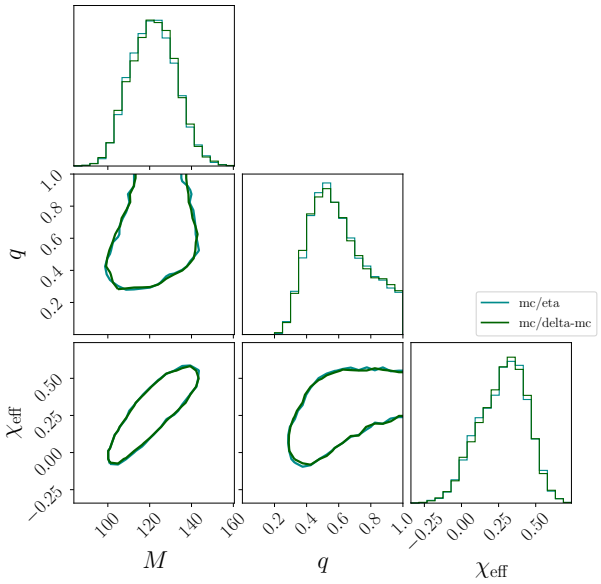

FIG. 4: RIFT analysis stability investigations: alternative coordinates. RIFT uses a specific coordinate system (and priors implemented in that coordinate system). If the structure of the fit is sensitive to smoothing effects or distortions imposed by the coordinate system or priors, alternative coordinates could identify these effects. No differences are seen.

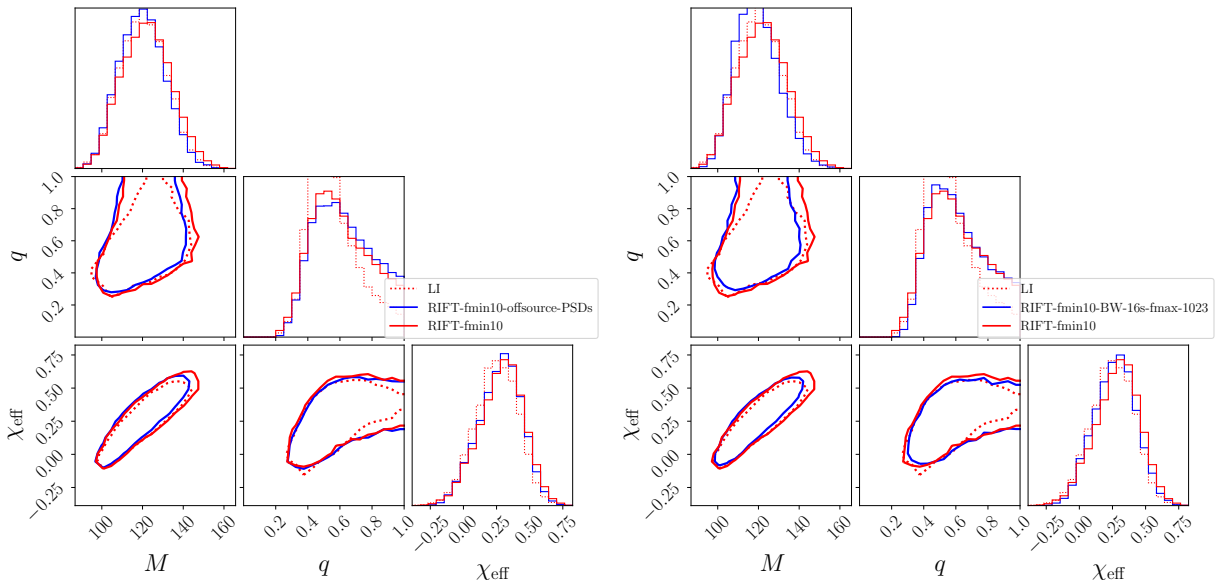

FIG. 5: RIFT analysis stability investigations using SEOBNRv4HM: reanalysis with alternative PSDs. The left panel compares an analysis with an alternative BW PSD to the fiducial SEOBNRv4HM RIFT and LI results; the right panel performs a similar comparison, but using an off-source PSD. This change produces very modest changes relative to our fiducial analysis. These changes are not sufficient to perturb the mass ratio distribution, relative to the changes needed to reproduce the LI result.

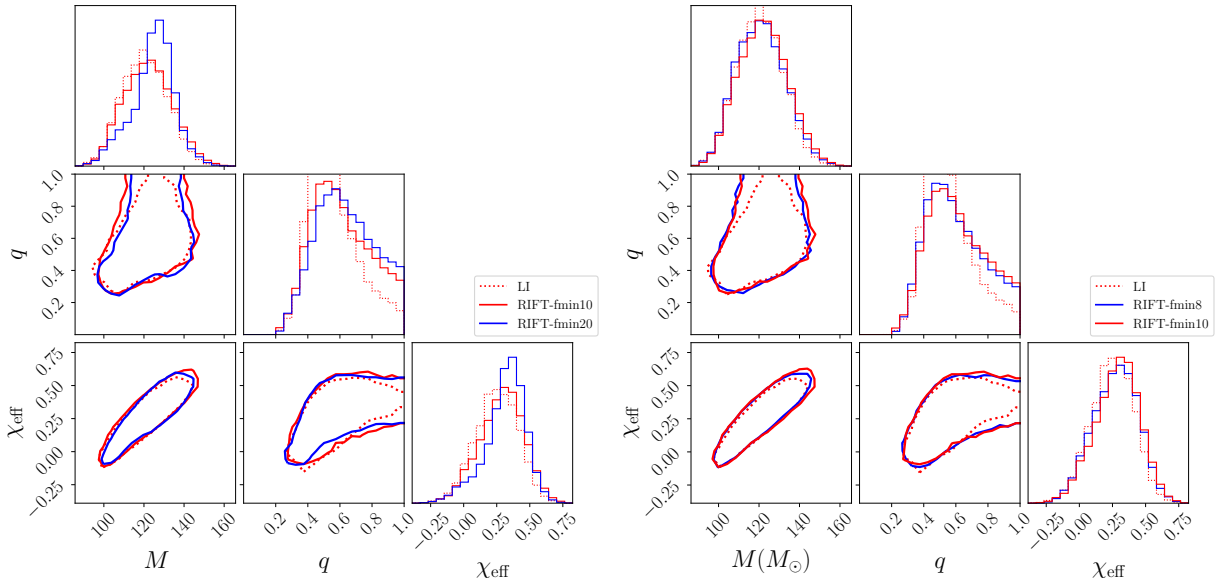

FIG. 6: RIFT analysis stability investigations using SEOBNRv4HM: reanalysis with alternative signal durations. For the right panel, where the starting frequency of the waveform is well below the starting frequency of the time integration, no differences are seen. For the left panel, the blue curve shows the effect of raising the starting waveform frequency to 20Hz, such that the higher modes start above 20 Hz. Even though this extreme change produces some differences relative to our fiducial analysis, they do not explain the differences seen in mass ratio.

they're applied to specific events. We defer future exploration and a detailed discussion of these differences to future work. Where available, RIFT results are provided at or linked from `https://github.com/oshaughn/RIFT_pe_public_samples`.

Acknowledgments

JL is supported by NSF PHY-1707965. RO'S is supported by NSF PHY-1707965 and PHY-1607520. We recognize K. Chatziioannou, S. Vitale, R. Cotesta, C. Haster, and CPL

Berry for their feedback, and K.C. for providing the BW PSDs used in this investigation.

APPENDIX A: RIFT NOTATION

The following text, duplicated from [20], is provided as a reference to inform discussion of tests of the RIFT algorithm and results.

ILE – a specific algorithm to "Integrate (the Likeilhood) over Extrinsic parameters" – provides a straightforward and efficient mechanism to compare any specific candidate gravitational wave source with real or synthetic data [11, 18, 19, 33], by marginalizing the likelihood of the data over the seven coordinates characterizing the spacetime coordinates and orientation of the binary relative to the earth. Specifically the likelihood of the data given gaussian noise, relative to gaussian noise, has the form (up to normalization)

$$\ln \mathcal{L}(\boldsymbol{\lambda}, \theta) = -\frac{1}{2}\sum_k \langle h_k(\boldsymbol{\lambda},\theta) - d_k | h_k(\boldsymbol{\lambda},\theta) - d_k\rangle_k - \langle d_k|d_k\rangle_k, \tag{A1}$$

where h_k are the predicted response of the kth detector due to a source with parameters ($\boldsymbol{\lambda}$, θ) and d_k are the detector data in each instrument k; $\boldsymbol{\lambda}$ denotes the combination of redshifted mass M_z and the remaining parameters needed to uniquely specify the binary's dynamics; θ represents the seven extrinsic parameters (4 spacetime coordinates for the coalescence event and 3 Euler angles for the binary's orientation relative to the Earth); and $\langle a|b\rangle_k \equiv \int_{-\infty}^{\infty} 2df \tilde{a}(f)^* \tilde{b}(f)/S_{h,k}(|f|)$ is an inner product implied by the kth detector's noise power spectrum $S_{h,k}(f)$. In practice we adopt both low- and high-frequency cutoffs $f_{\rm max}, f_{\rm min}$ so all inner products are modified to

$$\langle a|b\rangle_k \equiv 2\int_{|f|>f_{\rm min}, |f|<f_{\rm max}} df \frac{[\tilde{a}(f)]^* \tilde{b}(f)}{S_{h,k}(|f|)}. \tag{A2}$$

The joint posterior probability of $\boldsymbol{\lambda}, \theta$ follows from Bayes' theorem:

$$p_{\rm post}(\boldsymbol{\lambda},\theta) = \frac{\mathcal{L}(\boldsymbol{\lambda},\theta)p(\theta)p(\boldsymbol{\lambda})}{\int d\boldsymbol{\lambda} d\theta \mathcal{L}(\boldsymbol{\lambda},\theta)p(\boldsymbol{\lambda})p(\theta)}, \tag{A3}$$

where $p(\theta)$ and $p(\boldsymbol{\lambda})$ are priors on the (independent) variables $\theta, \boldsymbol{\lambda}$. For each $\boldsymbol{\lambda}$, we evaluate the marginalized likelihood

$$\mathcal{L}_{\rm marg} \equiv \int \mathcal{L}(\boldsymbol{\lambda},\theta)p(\theta)d\theta \tag{A4}$$

via direct Monte Carlo integration over almost all parameters θ, where $p(\theta)$ is uniform in 4-volume and source orientation. For the event time parameter, we marginalize by direct quadrature, for each choice of the remaining Monte Carlo parameters. For the remaining dimensions, to evaluate the likelihood in regions of high importance, we use an adaptive Monte Carlo as described in [11].

This marginalized likelihood can be evaluated efficiently by generating the dynamics and outgoing radiation in all possible directions once and for all for fixed λ, using a spherical harmonic decomposition. Using this cached information effectively, the likelihood can be evaluated as a function of θ at very low computational cost. A dimensionless, complex gravitational-wave strain

$$h(t,\vartheta,\phi;\lambda) = h_+(t,\vartheta,\phi;\lambda) - ih_\times(t,\vartheta,\phi;\lambda)\,, \tag{A5}$$

can be expressed in terms of its two fundamental polarizations h_+ and $h_\times$. Here, t denotes time, ϑ and ϕ are the polar and azimuthal angles for the direction of gravitational wave propagation away from the source. The complex gravitational-wave strain can be written in terms of spin-weighted spherical harmonics ${}_{-2}Y_{\ell m}(\vartheta,\phi)$ as

$$h(t,\vartheta,\phi;\lambda) = \sum_{\ell=2}^{\infty}\sum_{m=-\ell}^{\ell} \frac{D_{\rm ref}}{D} h^{\ell m}(t;\lambda) {}_{-2}Y_{\ell m}(\vartheta,\phi)\,, \tag{A6}$$

where the sum includes all available harmonic modes $h^{\ell m}(t;\boldsymbol{\lambda})$ made available by the model; where $D_{\rm ref}$ is a fiducial reference distance; and where D, the luminosity distance to the source, is one of the extrinsic parameters.

Following Pankow et al. [11], we substitute expression (A6) for $h_{\ell m}$ into the expression $h_k(t) = F_{+,k}h_+(t_k) + F_{\times,k}h_\times(t_k)$ for the detector response h_k, where $t_k = t_c - \vec{x}_k\cdot\hat{n}$ is the arrival time at the kth detector (at position $\vec{x}_k$) for a plane wave propagating along $\hat{n}$ [11]. We then substitute these expressions for h_k into the likelihood function (A1) thereby generating [11]

$$\begin{aligned}\ln \mathcal{L}(\lambda,\theta) = {} & (D_{\rm ref}/D){\rm Re}\sum_k\sum_{\ell m}(F_k {}_{-2}Y_{\ell m})^* Q_{k,lm}(\lambda,t_k) \\ & - \frac{(D_{\rm ref}/D)^2}{4}\sum_k\sum_{\ell m\ell' m'}\left[|F_k|^2[{}_{-2}Y_{\ell m}]^* {}_{-2}Y_{\ell' m'} U_{k,\ell m,\ell' m'}(\lambda) + {\rm Re}\left(F_k^2 {}_{-2}Y_{\ell m} {}_{-2}Y_{\ell' m'} V_{k,\ell m,\ell' m'}\right)\right]\end{aligned} \tag{A7}$$

where where $F_k = F_{+,k} - iF_{\times,k}$ are the complex-valued detector response functions of the kth detector [11] and the quantities Q, U, V depend on h and the data as

$$\begin{aligned} Q_{k,\ell m}(\lambda,t_k) &\equiv \langle h_{\ell m}(\lambda,t_k)|d\rangle_k \\ &= 2\int_{|f|>f_{\rm low}} \frac{df}{S_{n,k}(|f|)} e^{2\pi i f t_k}\tilde{h}^*_{\ell m}(\lambda;f)\tilde{d}(f)\,, \end{aligned} \tag{A8a}$$

$$U_{k,\ell m,\ell' m'}(\lambda) = \langle h_{\ell m}|h_{\ell' m'}\rangle_k\,, \tag{A8b}$$

$$V_{k,\ell m,\ell' m'}(\lambda) = \langle h^*_{\ell m}|h_{\ell' m'}\rangle_k\,. \tag{A8c}$$

Rewriting sums as matrix operations, the likelihood can be equivalently expressed as

$$\ln \mathcal{L} = \frac{D_{\rm ref}}{D}\mathrm{Re}[(FY)^\dagger Q] - \frac{D_{\rm ref}^2}{4D^2}[(FY)^\dagger UFY + (FY)^T VFY] \quad \text{(A9)}$$

where F, D are arrays over extrinsic parameters; Q is an array over time and (l, m); and U, V are matrices over (l, m).

[1] K. Chatziioannou and et al, Available as LIGO DCC P1900043 (2019).

[2] LIGO Scientific Collaboration, J. Aasi, B. P. Abbott, R. Abbott, T. Abbott, M. R. Abernathy, K. Ackley, C. Adams, T. Adams, P. Addesso, et al., Classical and Quantum Gravity **32**, 074001 (2015), 1411.4547.

[3] T. Accadia and et al, Journal of Instrumentation **7**, P03012 (2012), URL http://iopscience.iop.org/1748-0221/7/03/P03012.

[4] The LIGO Scientific Collaboration and the Virgo Collaboration, Phys. Rev. Lett **16**, 061102 (2016).

[5] B. Abbott et al. (The LIGO Scientific Collaboration and the Virgo Collaboration), Phys. Rev. X **6**, 041015 (2016), 1606.04856, URL https://journals.aps.org/prx/abstract/10.1103/PhysRevX.6.041015.

[6] B. P. Abbott, R. Abbott, T. D. Abbott, F. Acernese, K. Ackley, C. Adams, T. Adams, P. Addesso, R. X. Adhikari, V. B. Adya, et al., Physical Review Letters **118**, 221101 (2017), 1706.01812.

[7] The LIGO Scientific Collaboration, the Virgo Collaboration, B. P. Abbott, R. Abbott, T. D. Abbott, F. Acernese, K. Ackley, C. Adams, T. Adams, P. Addesso, et al., Phys. Rev. Lett **119**, 141101 (2017), 1709.09660.

[8] The LIGO Scientific Collaboration, the Virgo Collaboration, B. P. Abbott, R. Abbott, T. D. Abbott, F. Acernese, K. Ackley, C. Adams, T. Adams, P. Addesso, et al., Astrophysical Journal **851**, L35 (2017).

[9] The LIGO Scientific Collaboration, the Virgo Collaboration, B. P. Abbott, R. Abbott, T. D. Abbott, F. Acernese, K. Ackley, C. Adams, T. Adams, P. Addesso, et al., Phys. Rev. Lett **119**, 161101 (2017).

[10] The LIGO Scientific Collaboration, The Virgo Collaboration, B. P. Abbott, R. Abbott, T. D. Abbott, F. Acernese, K. Ackley, C. Adams, T. Adams, P. Addesso, et al., Available at https://dcc.ligo.org/LIGO-P1800307 and https://arxiv.org/abs/1811.12907 (2018).

[11] C. Pankow, P. Brady, E. Ochsner, and R. O'Shaughnessy, Phys. Rev. D **92**, 023002 (2015), URL http://adsabs.harvard.edu/abs/2015PhRvD..92b3002P.

[12] J. Lange, R. O'Shaughnessy, and M. Rizzo, Submitted to PRD; available at arxiv:1805.10457 (2018).

[13] J. Veitch, V. Raymond, B. Farr, W. M. Farr, P. Graff, S. Vitale, B. Aylott, K. Blackburn, N. Christensen, M. Coughlin, et al., Phys. Rev. D **91**, 042003 (2015), URL http://link.aps.org/doi/10.1103/PhysRevD.91.042003.

[14] B. P. Abbott, R. Abbott, T. D. Abbott, M. R. Abernathy, F. Acernese, K. Ackley, C. Adams, T. Adams, P. Addesso, R. X. Adhikari, et al., Living Reviews in Relativity **19**, 1 (2016).

[15] The LIGO Scientific Collaboration, (Available at https://dcc.ligo.org/LIGO-T1600115) (2016), URL https://dcc.ligo.org/LIGO-T1600115.

[16] The LIGO Scientific Collaboration, Available as https://dcc.ligo.org/LIGO-M1800085/public (2018), URL https://dcc.ligo.org/LIGO-M1800085/public.

[17] R. Smith and E. Thrane, Physical Review X **8**, 021019 (2018), 1712.00688.

[18] R. O'Shaughnessy, J. Blackman, and S. E. Field, Classical and Quantum Gravity **34**, 144002 (2017), 1701.01137.

[19] B. Abbott et al. (The LIGO Scientific Collaboration and the Virgo Collaboration), Phys. Rev. D **94**, 064035 (2016), URL http://link.aps.org/doi/10.1103/PhysRevD.94.064035.

[20] D. Wysocki, R. O'Shaughnessy, Y. Fang, and J. Lange, Submitted to PRD; available at http://arxiv.org/abs/1902.04934 (2019), paper source and examples available at https://github.com/oshaughn/ILE-GPU-Paper.git.

[21] R. O'Shaughnessy and J. Lange, *Rift source code*, available at https://github.com/oshaughn/research-projects-RIT.git.

[22] J. Blackman, S. E. Field, C. R. Galley, B. Szilágyi, M. A. Scheel, M. Tiglio, and D. A. Hemberger, Physical Review Letters **115**, 121102 (2015).

[23] J. Blackman, S. E. Field, M. A. Scheel, C. R. Galley, D. A. Hemberger, P. Schmidt, and R. Smith, Phys. Rev. D **95**, 104023 (2017), 1701.00550.

[24] J. Blackman, S. E. Field, M. A. Scheel, C. R. Galley, C. D. Ott, M. Boyle, L. E. Kidder, H. P. Pfeiffer, and B. Szilágyi, Phys. Rev. D **96**, 024058 (2017), 1705.07089.

[25] R. O'Shaughnessy and J. Lange, LIGO DCC T1800401 (2018).

[26] B. P. Abbott, R. Abbott, T. D. Abbott, M. R. Abernathy, F. Acernese, K. Ackley, C. Adams, T. Adams, P. Addesso, R. X. Adhikari, et al., Classical and Quantum Gravity **34**, 104002 (2017), 1611.07531, URL https://arxiv.org/abs/1611.07531.

[27] V. Varma, P. Ajith, S. Husa, J. C. Bustillo, M. Hannam, and M. Pürrer, Phys. Rev. D **90**, 124004 (2014).

[28] L. London, S. Khan, E. Fauchon-Jones, C. García, M. Hannam, S. Husa, X. Jiménez-Forteza, C. Kalaghatgi, F. Ohme, and F. Pannarale, Physical Review Letters **120**, 161102 (2018), 1708.00404.

[29] R. Cotesta, A. Buonanno, A. Bohé, A. Taracchini, I. Hinder, and S. Ossokine, Phys. Rev. D **98**, 084028 (2018), 1803.10701.

[30] J. Lange, R. O'Shaughnessy, and M. Rizzo (2017).

[31] N. J. Cornish and T. B. Littenberg, Classical and Quantum Gravity **32**, 135012 (2015), 1410.3835.

[32] The LIGO Scientific Collaboration, the Virgo Collaboration, B. P. Abbott, R. Abbott, T. D. Abbott, F. Acernese, K. Ackley, C. Adams, T. Adams, P. Addesso, et al., Submitted to PRX (2018).

[33] J. Lange, R. O'Shaughnessy, M. Boyle, J. Calderón Bustillo, M. Campanelli, T. Chu, J. A. Clark, N. Demos, H. Fong, J. Healy, et al., Phys. Rev. D **96**, 104041 (2017), 1705.09833.